Integrative and Comparative Biology

*Integrative and Comparative Biology*, volume 57, number 5, pp. 1055–1065
doi:10.1093/icb/icx099

*Society for Integrative and Comparative Biology*

SYMPOSIUM

# The Preoptic Area and the RFamide-Related Peptide Neuronal System Gate Seasonal Changes in Chemosensory Processing

Kimberly J. Jennings,[*] Manon Chasles,[†] Hweyryoung Cho,[*] Jens Mikkelsen,[†] George Bentley,[‡,§] Matthieu Keller[¶] and Lance J. Kriegsfeld[1,*,§]

[*]Department of Psychology, University of California, Berkeley, CA 94720, USA; [†]Department of Neurology and Neurobiology Research Unit, Blegdamsvej 9, DK-2100 Copenhagen, Denmark; [‡]Department of Integrative Biology, University of California, Berkeley, CA 94720, USA; [§]The Helen Wills Neuroscience Institute, University of California, Berkeley, CA 94720, USA; [¶]Physiologie de la Reproduction et des Comportements, UMR 0085 INRA, Centre Val-de-Loire, Nouzilly F-37380, France

From the symposium "Evolutionary Impacts of Seasonality" presented at the annual meeting of the Society for Integrative and Comparative Biology, January 4–8, 2017 at New Orleans, Louisiana.

[1]E-mail: kriegsfeld@berkeley.edu

**Synopsis** Males of many species rely on chemosensory information for social communication. In male Syrian hamsters (*Mesocricetus auratus*), as in many species, female chemosignals potently stimulate sexual behavior and a concurrent, rapid increase in circulating luteinizing hormone (LH) and testosterone (T). However, under winter-like, short-day (SD) photoperiods, when Syrian hamsters are reproductively quiescent, these same female chemosignals fail to elicit behavioral or hormonal responses, even after T replacement. It is currently unknown where in the brain chemosensory processing is gated in a seasonally dependent manner such that reproductive responses are only displayed during the appropriate breeding season. The goal of the present study was to determine where this gating occurred by identifying neural loci that respond differentially to female chemosignals across photoperiods, independent of circulating T concentrations. Adult male Syrian hamsters were housed under either long-day (LD) (reproductively active) or SD (reproductively inactive) photoperiods with half of the SD animals receiving T replacement. Animals were exposed to either female hamster vaginal secretions (FHVSs) diluted in mineral oil or to vehicle, and the activational state of chemosensory processing centers and elements of the neuroendocrine reproductive axis were examined. Components of the chemosensory pathway upstream of hypothalamic centers increased expression of FOS, an indirect marker of neuronal activation, similarly across photoperiods. In contrast, the preoptic area (POA) of the hypothalamus responded to FHVS only in LD animals, consistent with its role in promoting expression of male sexual behavior. Within the neuroendocrine axis, the RF-amide related peptide (RFRP), but not the kisspeptin neuronal system responded to FHVS only in LD animals. Neither response within the POA or the RFRP neuronal system was rescued by T replacement in SD animals, mirroring photoperiodic regulation of reproductive responses. Considering the POA and the RFRP neuronal system promote reproductive behavior and function in male Syrian hamsters, differential activation of these systems represents a potential means by which photoperiod limits expression of reproduction to the appropriate environmental context.

## Introduction

Species inhabiting temperate or boreal climates have adapted to survive winter through strict temporal regulation of reproduction, with the most energetically expensive phases of reproduction (e.g., lactation) restricted to times of year when resources are most abundant (i.e., spring). For Syrian hamsters (*Mesocricetus auratus*), reproduction is limited to long-day (LD) photoperiods of spring and summer and exposure to winter-like, short-day (SD) photoperiods drives reproductive quiescence (Gaston and Menaker 1967). Quiescence can be observed through gonadal regression (Zucker and Morin 1977), but also through alterations in the responsiveness to sexually-relevant chemosensory cues (Morin and Zucker 1978; Anand et al. 2002). The neural

Advance Access publication August 9, 2017

mechanisms by which photoperiod regulates chemosensory processing to limit reproduction to the appropriate season are currently unknown.

Female chemosignals (e.g., pheromones) elicit reproductive responses in males of many species (Nyby 2008; Liberles 2014), but male Syrian hamsters are especially reliant on chemosensory cues for social signaling. In the natural environment, solitary dwelling females scent mark using vaginal secretions to attract males to her burrow on the day of ovulation (Lisk et al. 1983). Female hamster vaginal secretions (FHVSs) are an "attractive" stimulus and exposure promotes expression of male sexual behavior (Murphy 1973; Johnston 1974; Darby et al. 1975). Lesions to either the main or accessory olfactory systems impair male sexual behavior (Murphy and Schneider 1970; Pfeiffer and Johnston 1994). In parallel to its behavior-promoting qualities, exposure to FHVS also stimulates a robust neuroendocrine response in the form of rapid release of luteinizing hormone (LH) and testosterone (T) (Macrides et al. 1974; Richardson et al. 2004).

In contrast to reproductively active males, hamsters housed under SD photoperiods fail to show either behavioral or neuroendocrine responses to these same chemosensory cues (Morin and Zucker 1978; Anand et al. 2002). Differences in responses to female chemosignals are not solely attributable to differences in circulating T. Expression of male sexual behavior is T-dependent (Whalen and Debold 1974; Powers and Bergondy 1983), and hamsters housed under SD photoperiods undergo gonadal regression and have correspondingly low concentrations of circulating T (Sisk and Turek 1983). However, T replacement is much less effective at restoring male sexual behavior in SD hamsters than in LD hamsters (Campbell et al. 1978; Morin and Zucker 1978; Miernicki et al. 1990; Pospichal et al. 1991). Thus, it is likely that photoperiod induces changes in the underlying neural substrates processing chemosignals to limit expression of reproductive responses to the appropriate season. The goal of the present study was to reveal these regulation centers by identifying neural loci that respond to female chemosignals differentially across photoperiods, and whose response in SD hamsters is not rescued by T replacement.

Photoperiod could impact chemosensory processing at any point in the chemosensory pathway, from early sensory processing by the main and accessory olfactory systems through integration by the medial amygdala (Coolen and Wood 1998; Petrulis 2013). Alternatively, early processing may remain consistent across photoperiods, but differences in downstream hypothalamic target structures may gate behavioral or neuroendocrine output. To test these hypotheses, the present study examined induction of FOS, the protein product of the immediate early gene *cfos* and indirect marker of neuronal activation, along the chemosensory pathway from sensory input to hypothalamic targets (Fiber et al. 1993; Petrulis 2013), in response to FHVS.

Considering the robust neuroendocrine component of male responses to female chemosignals, gating of chemosensory processing may also occur within elements of the neuroendocrine reproductive axis. Although chemosignal-induced increases in LH are presumed to be driven by upstream release of gonadotropin releasing hormone (GnRH), neither expression of GnRH mRNA nor rates of GnRH/FOS coexpression are altered by acute conspecific pheromonal stimulation (Gore et al. 2000; Richardson et al. 2004; Taziaux and Bakker 2015). The neuropeptide kisspeptin is expressed within neurons of the anteroventral periventricular nucleus (AVPV) and arcuate nucleus of the hypothalamus and potently stimulates GnRH release (de Roux et al. 2003; Irwig et al. 2004; Lehman et al. 2013). Whereas the AVPV kisspeptin population projects directly to GnRH cell bodies (Yeo and Herbison 2011), the arcuate kisspeptin cell population acts on GnRH terminals in the mediobasal hypothalamus to facilitate GnRH release without necessitating changes in GnRH cell firing rate (or FOS coexpression) (d'Anglemont de Tassigny et al. 2008). The arcuate kisspeptin system has also been implicated in mediating male chemosignal-induced increases in LH in female goats (De Bond et al. 2013; Jouhanneau et al. 2013; Sakamoto et al. 2013). Thus, we also examined these populations of kisspeptin cells as possible loci at which female chemosignals act to increase LH release.

In addition to kisspeptin, the neuropeptide RFamide-related peptide (RFRP; the mammalian ortholog of avian gonadotropin inhibitory hormone [GnIH]) also potently regulates release of GnRH and is sensitive to social context (Kriegsfeld et al. 2006; Calisi et al. 2011; Tobari et al. 2014; Jennings et al. 2016). In male Syrian hamsters, RFRP stimulates release of LH in both LD and SD photoperiods (Ancel et al. 2012), although the stimulatory nature of this effect is sex (Kriegsfeld et al. 2006) and species specific (Ubuka et al. 2012). Interestingly, RFRP may also directly regulate release of LH by the anterior pituitary through projections to the median eminence (Tsutsui et al. 2000; Kriegsfeld et al. 2006; Smith et al. 2012), suggesting an alternative pathway for chemosensory regulation of neuroendocrine

function. Finally, expression of RFRP is also strongly regulated by photoperiod, independent of changes in gonadal steroids (Revel et al. 2008; Mason et al. 2010), pointing to a potential role in integrating social and photoperiodic information to gate chemosensory responses.

## Materials and methods

### Animals

Adult (56 days of age, $n = 37$) male Syrian hamsters (*M. auratus*; LVG (SYR)) obtained from Charles River (Wilmington, MA) were maintained on a 14:10 h light:dark cycle (LD, lights off 22:00 Pacific Standard Time [PST]) upon arrival. After a 10 day acclimation period, 23 hamsters were transferred to a 10:14 h light:dark cycle (SD, lights off 20:00 PST) and 14 remained in the LD photoperiod. Five adult (>60 days of age) female Syrian hamsters were housed under a 14:10 h light:dark cycle to supply FHVS. Hamsters were singly housed at $23 \pm 1\,^{\circ}C$ in polypropylene cages ($48 \times 25 \times 21$ cm) furnished with Tek-Fresh Lab Animal Bedding (Harlan Teklab, Madison, WI). Tap water and Lab Diet Prolab 5P00 were available *ad libitum*. All procedures were approved by the Animal Care and Use Committee of the University of California at Berkeley and conformed to principles enumerated in the NIH guide for the use and care for laboratory animals.

Twelve weeks after transfer into SD photoperiod, 12 SD animals received subcutaneous Silastic capsules (1.98 mm I.D., 3.18 O.D.; Dow Corning, Midland, MI) containing crystalline testosterone propionate (TP) (20 mm TP bounded by 3 mm silicone sealant at each end, Sigma Aldrich, St Louis, MO) whereas remaining animals ($n = 11$ SD, $n = 14$ LD) received empty capsules, yielding three groups (LD, SD, SD + T). To implant capsules, hamsters were anesthetized with isoflurane vapors (3%; Clipper Distributing Company, St Joseph, MO) and capsules were inserted through a small midline incision in the nape of the neck. Silastic capsules were primed prior to implantation by submersion in 0.9% saline for 24 h, and yield plasma T concentrations within the physiological range for this species (Campbell et al. 1978). Hamsters received buprenorphine (0.1 mg/kg; Hospira, Lake Forest, IL) subcutaneously for postoperative analgesia.

### FHVS exposure

Nine to eleven days after implantation of Silastic capsules, half of the animals in each group ($n = 7$ LD, 6 SD, 6 SD + T) were exposed to FHVS whereas the other half ($n = 7$ LD, 5 SD, 6 SD + T) were exposed to vehicle. FHVSs were collected from intact, cycling females on the morning of estrus over the week preceding exposure and stored at $-20\,^{\circ}C$. FHVSs were thawed shortly before exposure, diluted 1:2 with mineral oil, and kept on ice until use. Hamsters were weighed during the light phase approximately 12 h before exposure and assigned to a stimulus groups. Exposure was achieved by applying approximately 20 µL of diluted FHVS or vehicle directly to the snout using a standard laboratory spatula. Separate spatulas were used for FHVS and vehicle, and tools were cleaned with 70% ethanol between animals. All exposures occurred between 1 and 4 h after lights off (i.e., early part of the dark/active phase) under dim red light. Hamsters were then left undisturbed for 1 h before being transferred to another room for perfusion.

### Perfusion and immunohistochemistry

Hamsters were deeply anesthetized with sodium pentobarbital solution (200 mg/kg) and perfused transcardially with 100 mL 0.9% saline followed by 300 mL 4% paraformaldehyde in 0.1 M phosphate buffered saline (PBS) (pH 7.3). Paired testes, epididymis, brown adipose tissue (BAT), and epididymal white adipose tissue (EWAT) were collected and weighed to confirm animals had responded to SD photoperiod with gonadal regression appropriately. Brains were postfixed for 3 h in 4% paraformaldehyde followed by cryoprotection in 30% sucrose in 0.1 M PBS for 48 h. Brains were then frozen at $-80\,^{\circ}C$ until processed. A total of 40 µm coronal brain sections were collected on a Leica 2050S cryostat at $-20\,^{\circ}C$. Slices were stored at $-20\,^{\circ}C$ in an ethylene glycol and sucrose based antifreeze until immunohistochemistry was performed.

To visualize the expression of FOS as well as the colocalization of FOS with kisspeptin or RFRP, double-label immunofluorescence was performed on separate sets of every fourth 40 µm brain section. Free floating sections were washed in PBS, incubated for 10 min in 0.5% hydrogen peroxide, washed in PBS again, and then blocked for 1 h in 2% normal goat serum suspended in 0.1% Triton X-100 (PBT). Sections were then incubated for 48 h at $4\,^{\circ}C$ in either a rabbit polyclonal anti-GnIH antibody (1:120,000; PAC 123/124, Dr George Bentley) or a rabbit polyclonal anti-kisspeptin antibody (1:2000; Dr Jens Mikkelsen) with 1% normal goat serum in PBT. After incubation in the primary antibody, sections were washed in PBT, incubated for 1 h in biotinylated goat anti-rabbit IgG (1:250, Vector

Laboratories, Burlingame, CA), 1 h in avidin–biotin–horseradish peroxidase complex (ABC Elite Kit, Vector Laboratories), and 30 min in 0.6% biotinylated tyramide solution, with PBT washes in between each step. After washing with PBS, cells were fluorescently labeled with CY-2 strepdavidin conjugate (1:150, Jackson ImmunoResearch Laboratories, West Grove, PA) and washed with PBS again. Next, sections incubated for 48 h at 4 °C with a rabbit anti-FOS primary antibody (1:10,000; sc-52, Santa Cruz Biotechnology, Dallas, TX) and 1% normal donkey serum in PBT. Sections were then washed with PBT and labeled with the fluorophore CY-3 donkey-anti-rabbit (1:150, Jackson ImmunoResearch Laboratories, West Grove, PA). Finally, sections were washed with PBS and counterstained with Hoechst (for Kisspeptin/FOS) or 4′,6-diamidino-2-phenylindole (DAPI) (for RFRP/FOS).

### Microscopy and quantification

Sections were examined at the conventional light microcopy level using the standard wavelengths for CY-2 (488 nm), CY-3 (568 nm), and DAPI/Hoechst (358 nm) with a Zeiss Z1 microscope (Thornwood, NY). Each label was captured as a single image at ×200 magnification without adjusting the plane of focus between captures and then superimposed digitally. Brain areas were examined by observers blind to the experimental conditions using Image J (NIH) to view the three channels independently or together.

Expression of FOS was manually quantified within the piriform cortex (anterior, median, posterior), septum, ventromedial hypothalamus (VMH), medial amygdala (postero-dorsal, MeApd, and postero-ventral, MeApv), anterior cortical amygdala (ACo), preoptic area (POA), bed nucleus of the stria terminalis (BNST), the accessory olfactory bulb (AOB) (granular and mitral layers), and the main olfactory bulb (MOB) granular layer using sections double labeled for kisspeptin and FOS. Every fourth section through the dorsomedial hypothalamus (DMH) was examined for colocalization of RFRP and FOS, and every fourth section through the AVPV was examined for colocalization of kisspeptin and FOS. Neuroanatomical regions were defined by reference to a published Syrian hamster atlas (Morin and Wood 2001). A cell was considered to be double labeled if FOS was expressed in the nucleus without extending beyond its predetermined borders. Cells without a clearly identifiable nucleus were not included in analysis.

A second population of kisspeptin cells is also found in the arcuate nucleus, but cell bodies are not able to be visualized without pretreatment with colchicine to reduce fiber density. As a result, arcuate kisspeptin/FOS coexpression was not examined in this study. Instead, kisspeptin-immunoreactive (-ir) fiber density was quantified using a previously published approach (Losa et al. 2011). Briefly, images of kisspeptin-ir fibers were taken at ×400 magnification from one section each corresponding to the anterior, median, and posterior arcuate nucleus. Images were then binarized and depixelated to minimize background, and fibers were skeletonized to a thickness of 1 pixel to control for variation in fiber thickness and brightness. The resulting pixels were quantified using the Image J Voxel Counter plug-in (NIH) and are reported as mean volume, or the proportion of voxels identified to contain kisspeptin-ir fibers.

### Statistics

All statistical analyses were performed using GraphPad Prism 6.0 (GraphPad Software, La Jolla, CA). FOS colocalization data were arcsine transformed prior to analysis to meet assumptions of normality. Data (regional FOS expression; RFRP and kisspeptin cell counts; and FOS co-localization) were analyzed using two-way analyses of variance (ANOVAs) for each variable with stimulus (FHVS or vehicle) and photoperiod (LD, SD, or SD + T) as factors. If the ANOVA revealed a main effect of photoperiod, Tukey's tests were used to probe group differences. If the ANOVA revealed a significant interaction effect, planned comparisons using Fisher's LSD test were performed to examine the effect of FHVS compared with vehicle within each photoperiodic group. All results were considered statistically significant if $P < 0.05$.

## Results

### Confirmation of responsiveness to photoperiod exposure

As expected, animals exposed to SD photoperiods experienced gonadal regression and presented with smaller reproductive tissues than their LD counterparts. Body and tissue weights on the day of chemosensory exposure are listed in Table 1. Two-way ANOVAs revealed main effects of photoperiod for paired testes ($F_{(2,\ 29)} = 29.80$, $P < 0.001$), paired epididymis ($F_{(2,\ 29)} = 19.68$, $P < 0.001$), and EWAT ($F_{(2,\ 29)} = 6.45$, $P < 0.01$) weights. In all cases, both SD and SD + T animals have lower tissue weights than LD animals (Tukey's test; LD versus SD and LD versus SD + T $P < 0.05$, SD versus SD + T $P > 0.05$). There were no effects of photoperiod on body mass or BAT weights ($P > 0.05$ in both cases).

**Table 1** Body and tissue weights on day of chemosensory exposure

| | LD | | | | | | SD | | | | | | SD+T | | | | | |
|---|---|---|---|---|---|---|---|---|---|---|---|---|---|---|---|---|---|---|
| | Vehicle | | | FHVS | | | Vehicle | | | FHVS | | | Vehicle | | | FHVS | | |
| Tissue weight (g) | Mean | SEM | *n* | Mean | SEM | *n* | Mean | SEM | *n* | Mean | SEM | *n* | Mean | SEM | *n* | Mean | SEM | *n* |
| Body weight | 194.1 | 8.5 | 7 | 197 | 7.5 | 7 | 186.6 | 9.9 | 5 | 164.9 | 12.8 | 6 | 191.3 | 5.2 | 6 | 176.5 | 15.6 | 6 |
| Paired testes* | 3.1 | 0.3 | 7 | 2.3 | 0.4 | 7 | 0.5 | 0.1 | 5 | 0.4 | 0.0 | 6 | 1.1 | 0.5 | 5 | 0.7 | 0.2 | 5 |
| Paired epididymis* | 1.2 | 0.1 | 7 | 1.0 | 0.2 | 7 | 0.4 | 0.1 | 5 | 0.3 | 0.0 | 6 | 0.6 | 0.2 | 5 | 0.4 | 0.1 | 5 |
| BAT | 0.5 | 0.0 | 7 | 0.5 | 0.1 | 7 | 0.5 | 0.0 | 5 | 0.4 | 0.0 | 6 | 0.4 | 0.0 | 5 | 0.5 | 0.1 | 5 |
| EWAT* | 5.9 | 0.7 | 7 | 5.7 | 0.5 | 7 | 4.1 | 0.7 | 5 | 3.2 | 0.7 | 6 | 4.1 | 0.5 | 5 | 4.2 | 0.9 | 5 |

*Denotes main effect of photoperiod $P < 0.05$.

There were no effects of stimulus or interactions between stimulus and photoperiod for any somatic weights ($P > 0.05$ in all cases).

### FOS induction along the chemosensory pathway

Regional expression of FOS, an indirect protein marker of recent neuronal activation, in only two regions, the granular layer of the AOB and the POA, revealed a statistically significant interaction effect (AOB granular layer $F_{(2,\ 23)} = 6.43$, $P < 0.01$; POA $F_{(2,\ 30)} = 3.52$, $P = 0.04$) (Table 2). Planned comparisons revealed that FHVS exposure increased the number of FOS-ir cells in this region only within LD animals ($P = 0.04$), whereas no difference between FHVS and vehicle groups was detected within SD or SD + T animals ($P > 0.05$) (Fig. 1). In contrast, no differences between vehicle and FHVS were found within LD and SD groups for the AOB granular layer ($P > 0.05$), but FHVS exposure increased FOS expression in this region within the SD + T cohort ($P < 0.01$) (Table 2). For all other regions along the chemosensory pathway, the magnitude of FOS induction following FHVS exposure was grossly similar across photoperiods. ANOVAs revealed either a main effect of stimulus (ACo $F_{(1,\ 27)} = 9.756$, $P < 0.01$; MeApd $F_{(1,\ 27)} = 7.227$, $P = 0.01$; MeApv $F_{(1,\ 26)} = 10.47$, $p < 0.01$; VMH $F_{(1,\ 30)} = 5.201$, $p = 0.03$) or no effects on the number of FOS-ir cells. In no cases was a main effect of photoperiod discovered ($P > 0.05$ in all cases).

### Responses within the reproductive axis

Total cell number and the proportion of cells colocalizing FOS was quantified for RFRP (within the DMH), and kisspeptin (within the AVPV) immunoreactive (-ir) cells. Additionally, kisspeptin-ir fiber density was quantified at three levels of the arcuate nucleus (anterior, median, and posterior). Of these metrics, an ANOVA revealed a significant interaction between stimulus and photoperiod only for the total number of RFRP-ir cells ($F_{(2,\ 31)} = 4.790$, $P = 0.02$), with the number of cells reduced following FHVS exposure compared with vehicle exposure only within LD animals (Fisher's LSD $P < 0.001$) but not within either SD or SD + T animals ($P > 0.05$ in both cases) (Fig. 2A). In contrast, the proportion of RFRP-ir cells co-expressing FOS did not vary across groups ($P > 0.05$ for all ANOVA terms) (Fig. 2B).

Photoperiod-driven changes in RFRP immunoreactivity have been reported previously (Mason et al. 2010) and were replicated in the present study. A main effect of photoperiod was found for RFRP-ir cell number ($F_{(2,\ 31)} = 22.60$, $P < 0.001$), with LD animals overall displaying more RFRP-ir cells than both SD and SD + T animals, with SD + T animals similarly displaying more cells than SD animals (Tukey's test, $P < 0.05$ in each case) (Fig. 2A). Kisspeptin immunoreactivity has also been reported to vary across photoperiods in this species (Clarke and Caraty 2013), but in the present study, effects of both photoperiod and stimulus failed to reach statistical significance (Fig. 3). Only two AVPV kisspeptin-ir cells were found to co-express FOS (one cell each in a LD/FHVS and SD + T/Vehicle animal), so statistical differences in this measure were not analyzed.

## Discussion

The present study sought to identify regions or cell types in the brain that restrict expression of reproductive responses to female chemosignals to the appropriate season, identified by their differential responses to FHVS across photoperiods. Analysis of neuronal activation in early chemosensory processing centers indicates that early sensory processing remains consistent across photoperiods, suggesting that photoperiodic regulation of downstream structures is critical for differences seen in reproductive output. Indeed, downstream chemosensory targets of

**Table 2** Number of FOS-ir cells in regions of the chemosensory pathway following stimulus exposure

| | LD | | | | | | SD | | | | | | SD+T | | | | | |
|---|---|---|---|---|---|---|---|---|---|---|---|---|---|---|---|---|---|---|
| | Vehicle | | | FHVS | | | Vehicle | | | FHVS | | | Vehicle | | | FHVS | | |
| Region | Mean | SEM | *n* | Mean | SEM | *n* | Mean | SEM | *n* | Mean | SEM | *n* | Mean | SEM | *n* | Mean | SEM | *n* |
| MOB granular layer | 99.9 | 13.2 | 6 | 83.9 | 16.2 | 7 | 62.5 | 7.8 | 3 | 99.4 | 16.7 | 5 | 74.4 | 7.4 | 4 | 97.9 | 12.2 | 6 |
| AOB granular layer* | 115.1 | 25.1 | 5 | 100.8 | 12.8 | 7 | 132.8 | 22.8 | 2 | 93.0 | 8.2 | 5 | 67.0 | 16.2 | 4 | 150.2** | 15.3 | 6 |
| AOB mitral layer | 28.6 | 5.1 | 5 | 29.9 | 2.3 | 7 | 14.5 | 3.5 | 2 | 22.3 | 3.6 | 5 | 21.8 | 5.2 | 4 | 30.9 | 4.7 | 6 |
| Pyriform cortex—anterior | 21.3 | 8.2 | 7 | 54.4 | 25.3 | 5 | 27.4 | 11.4 | 5 | 63.5 | 26.2 | 6 | 34.4 | 12.8 | 5 | 43.7 | 19.5 | 6 |
| Pyriform cortex—median | 29.4 | 14.2 | 7 | 71.6 | 24.8 | 7 | 33.4 | 10.7 | 5 | 69.3 | 29.4 | 6 | 61.2 | 28.2 | 6 | 29.7 | 8.8 | 6 |
| Pyriform cortex—posterior | 22.1 | 7.0 | 7 | 58.6 | 19.0 | 7 | 41.8 | 13.9 | 5 | 62.7 | 15.4 | 6 | 39.8 | 11.0 | 5 | 33.0 | 12.5 | 6 |
| ACo*** | 7.7 | 3.8 | 6 | 16.4 | 7.5 | 7 | 7.6 | 3.3 | 5 | 40.5 | 12.7 | 6 | 20.2 | 10.6 | 5 | 51.5 | 15.8 | 4 |
| BNST | 15.7 | 3.6 | 7 | 23.9 | 6.7 | 7 | 16.8 | 8.1 | 5 | 25.7 | 5.6 | 6 | 18.0 | 5.0 | 6 | 14.2 | 4.8 | 6 |
| MeApd*** | 6.7 | 2.6 | 6 | 24.3 | 7.1 | 7 | 8.6 | 2.9 | 5 | 25.0 | 8.9 | 5 | 17.0 | 9.2 | 5 | 35.6 | 13.3 | 5 |
| MeApv*** | 4.5 | 1.2 | 6 | 17.3 | 5.1 | 6 | 15.0 | 5.9 | 5 | 37.2 | 10.8 | 6 | 7.8 | 3.0 | 4 | 22.4 | 3.3 | 5 |
| POA* | 25.6 | 4.8 | 7 | 55.3** | 17.5 | 7 | 24.0 | 7.2 | 5 | 37.2 | 3.7 | 5 | 56.2 | 8.7 | 6 | 33.0 | 9.0 | 6 |
| Septum | 2.6 | 0.9 | 7 | 6.6 | 3.9 | 7 | 2.4 | 1.7 | 5 | 5.2 | 2.2 | 6 | 5.7 | 2.7 | 6 | 2.5 | 0.8 | 6 |
| VMH*** | 5.1 | 2.3 | 7 | 6.6 | 2.6 | 7 | 5.2 | 1.6 | 5 | 13.5 | 3.6 | 6 | 3.6 | 1.0 | 5 | 10.2 | 4.2 | 6 |

*Denotes interaction between stimulus and photoperiod $P < 0.05$.
**Denotes $P < 0.05$ compared with vehicle control in the same photoperiodic group.
***Denotes main effect of stimulus $P < 0.05$.

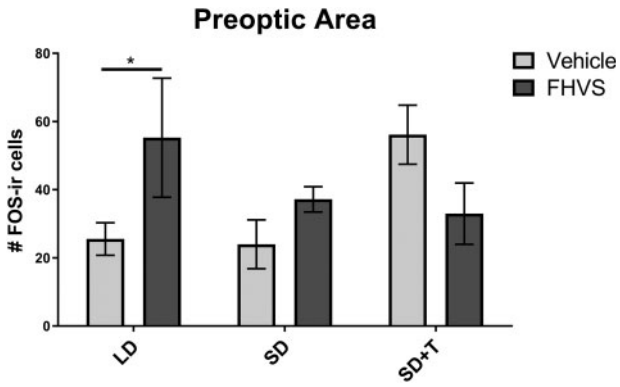


**Fig. 1** Mean (±SEM) number of FOS-ir cells in the POA. Asterisk (*) denotes $P < 0.05$ comparing vehicle with FHVS exposed animals.

the POA of the hypothalamus and RFRP-ir cells within the DMH both respond to female chemosignals within LD but not SD hamsters. The POA and RFRP neuronal system promote reproductive behavior and function, respectively, in male Syrian hamsters (Hull and Dominguez 2007; Ancel et al. 2012). Importantly, responses within SD hamsters are not rescued by T replacement, mirroring previous reports of the inability of T replacement to rescue male sexual behavior under SD photoperiod (Campbell et al. 1978; Morin and Zucker 1978; Miernicki et al. 1990; Pospichal et al. 1991). Taken together, these data suggest that photoperiod acts on the POA and RFRP neuronal system in a T-independent manner, contributing to the gating of chemosensory responsiveness in SD photoperiods (Fig. 4).

Despite differences in behavioral and neuroendocrine output in response to FHVS, neuronal activation of early chemosensory processing centers (e.g., MOB, ACo, BNST, MeA), as indirectly measured by FOS expression, does not vary across photoperiods and concentrations of circulating T. The significant interaction between stimulus and photoperiod seen for the AOB granular layer presents a notable exception to this statement. It is unclear why animals of the SD + T group would have a more robust response to FHVS than their SD or LD counterparts. However, it is unlikely this finding has strong biological significance in the present context, given that SD + T animals are similar to SD animals in their behavioral responses to the stimulus (Campbell et al. 1978; Morin and Zucker 1978; Miernicki et al. 1990; Pospichal et al. 1991). Overall, these findings are consistent with previous reports that detection of, and neural responses to, FHVS do not require high circulating T (Fiber and Swann 1996; Swann 1997; Romeo et al. 1998; Peters et al. 2004). However, exposure to SD photoperiod is independently associated with changes in sensitivity to steroid hormones and with morphological changes in many chemosensory processing centers (see Kriegsfeld and Bittman [2009] for review). Thus, it is possible that photoperiod-driven alterations to these structures

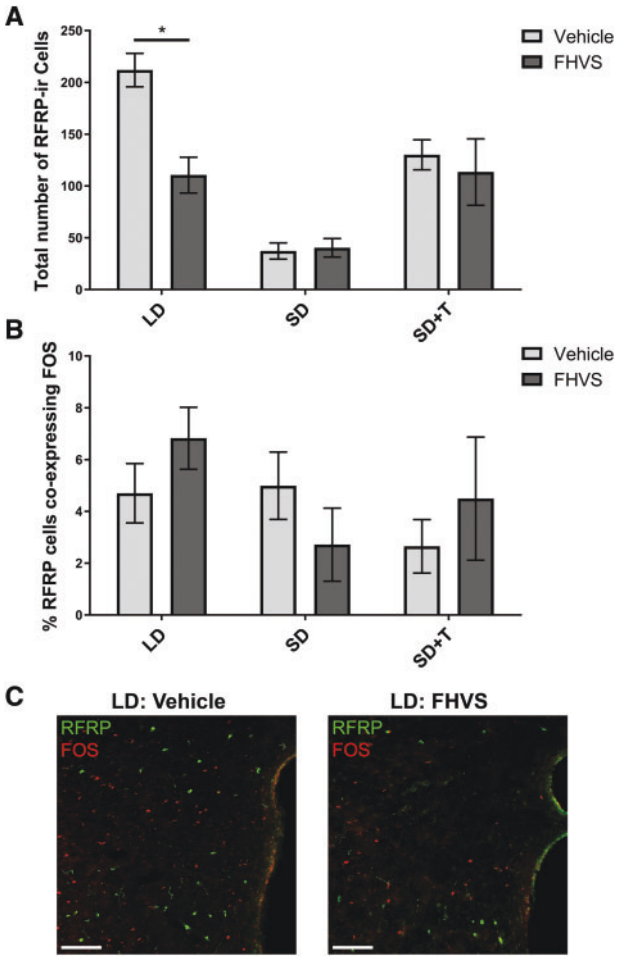


**Fig. 2** (**A**) Mean (±SEM) number of RFRP-ir cells in the DMH. (**B**) Mean (±SEM) percentage of RFRP-ir cells co-expressing FOS. (**C**) Representative photomicrographs depicting RFRP-ir and FOS-ir cells in LD animals exposed to vehicle (left) or FHVS (right). In the online version of the manuscript, RFRP-ir cells are depicted in green and FOS-ir cells in red. Scale bar represents 100 µm. * denotes $P < 0.05$ comparing vehicle to FHVS exposed animals.

might contribute to differential responsiveness to female chemosignals. Results of the current study suggest that any such photoperiod-driven changes within chemosensory centers do not interfere with neuronal activation by female chemosignals.

The POA is a major target of the chemosensory system and is essential for the expression of male sexual behavior (Coolen and Wood 1998; see Hull and Dominguez [2007] for review). The POA is a critical integration center of chemosensory and hormonal information, with removal of either input type to this region abolishing copulation (Wood and Newman 1995). In the present study, exposure to FHVS increases neuronal activation in this region in LD but not SD animals, consistent with a role in gating reproductive behavior. Induction of FOS after FHVS exposure within the POA has been reported to require T (Swann 1997). However, our findings indicate that chemosensory activation of this region is not rescued by T replacement in SD animals, further paralleling regulation of behavior across photoperiods (Morin and Zucker 1978). Future research will be necessary to explore the specific mechanisms by which photoperiod regulates POA function to gate responsiveness to female chemosignals.

As mentioned previously, exposure to female chemosignals elicits a rapid increase in LH and T in LD hamsters, presumably to facilitate reproductive behavior and function upon encountering a potential mate (Anand et al. 2002; Richardson et al. 2004; Nyby 2008). Investigation of the kisspeptin and RFRP systems, both potent upstream regulators of GnRH and LH release in male Syrian hamsters, revealed RFRP to be differentially responsive to female chemosignals across photoperiods. The number of RFRP-ir cells decreased 1 h after FHVS exposure in LD but not SD animals, and this response was not rescued by T replacement. To our knowledge, this is the first report that the RFRP neuronal system is sensitive to chemosensory information. These data are consistent with building evidence that RFRP mediates social modulation of reproduction (Calisi et al. 2011; Tobari et al. 2014; Jennings et al. 2016; Peragine et al. 2017). In male Syrian hamsters, unlike many other mammalian species, RFRP acts to stimulate release of LH under both LD and SD photoperiods (Ancel et al. 2012). Thus, the acute decrease in RFRP-ir cell number observed in the present study may reflect acute release of the RFRP peptide, facilitating LH release in LD males in response to female chemosignals. A rapid release of the RFRP peptide would reduce the amount of peptide detectable with immunohistochemistry, leading to a reduction in total cell numbers. Changes in post-translational regulation cannot be excluded, but seem unlikely considering the rapid timecourse (1 h) and robust decrease (~50%). If true, the reduced detection of activated RFRP-ir neurons might also explain the absence of statistically significant changes in the proportion of RFRP-ir cells coexpressing FOS in response to FHVS. Regardless, these data point to the RFRP neuronal system as an important integration center for chemosensory and photoperiodic information. Expression of RFRP mRNA and peptide is regulated by photoperiod (Revel et al. 2008; Mason et al. 2010), and the high density of melatonin receptors in the DMH suggests RFRP neurons may be directly sensitive to photoperiod-driven changes in melatonin secretion (Maywood et al. 1996; Ubuka et al. 2005). Input onto RFRP neurons has not been extensively mapped, so it is unclear

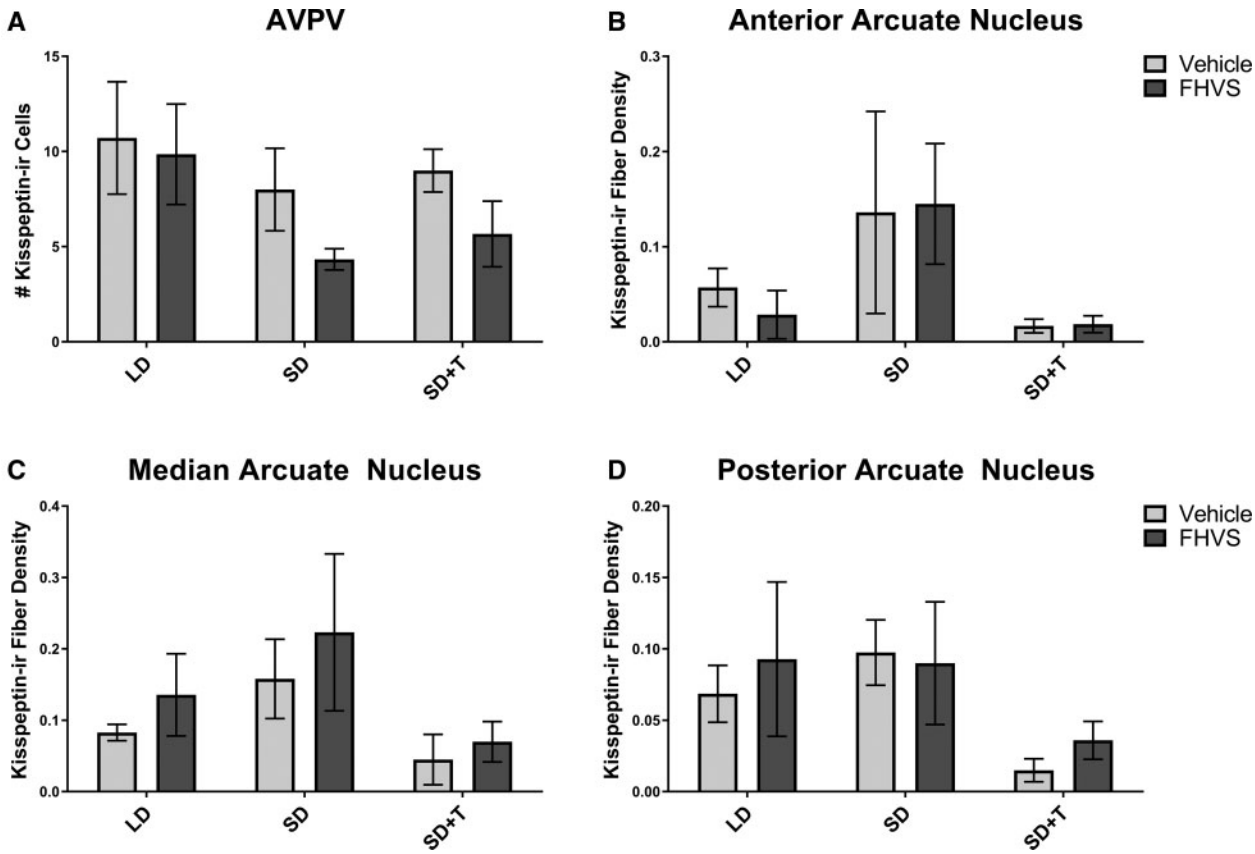


**Fig. 3** (**A**) Mean (±SEM) number of kisspeptin-ir cells in the AVPV. (**B**) Mean (±SEM) volume of kisspeptinir fibers in the anterior arcuate nucleus. (**C**) Mean (±SEM) volume of kisspeptin-ir fibers in the median arcuate nucleus. (**D**) Mean (±SEM) volume of kisspeptin-ir fibers in the posterior arcuate nucleus.

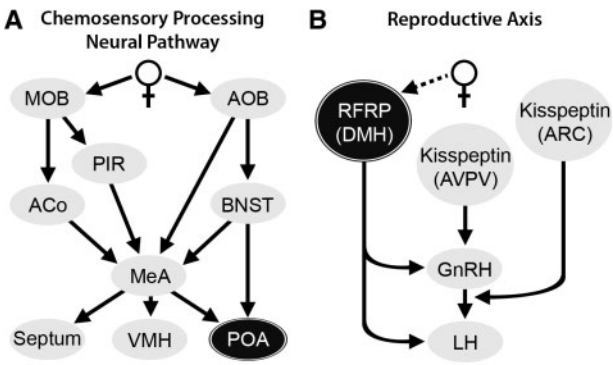


**Fig. 4** Summary of present findings. (**A**) Diagram of neural loci through which chemosensory information is processed. Unlike upstream chemosensory processing loci, the response of the POA to chemosensory information is modulated by photoperiod, represented by dark shading. Symbol ♀ represents chemosensory information, i.e., FHVS. (**B**) Diagram of the neuroendocrine reproductive axis. The RFRP neuronal system is sensitive to chemosensory information, and this response is modulated by photoperiod. The dotted line indicates that the pathway by which chemosensory information is transmitted to the RFRP neuronal system remains to be established.

whether RFRP neurons receive direct input from chemosensory loci and whether any such afferents are modulated by photoperiod.

Photoperiodic modulation of RFRP neuronal responses to female chemosignals may also contribute to differences in evoked behavior. RFRP's actions on LH release are species and sex specific (Kriegsfeld et al. 2006; Ancel et al. 2012; Ubuka et al. 2012). RFRP inhibits sexual behavior in species/sexes in which RFRP also inhibits LH release (Bentley et al. 2006; Johnson et al. 2007; Piekarski et al. 2013; Ubuka et al. 2014). RFRP-ir neurons project to brain regions outside the neuroendocrine reproductive axis, suggesting a wider neuromodulatory role (Kriegsfeld et al. 2006). Relevant to the present investigation, RFRP neurons project to the POA, and chronic infusion of RFRP in female Syrian hamsters both reduced sexual behavior and altered expression of FOS in the POA, independent of downstream effects on sex steroids (Piekarski et al. 2013).

Findings in ungulates have implicated the kisspeptin population of the arcuate nucleus in mediating

male pheromone-induced increases in LH within females. Exposure to male chemosignals causes an increase in multiunit activity recorded in close proximity to arcuate kisspeptin cells coupled to increases in LH, and the male chemosignal-induced rise in LH is blocked by infusion of a kisspeptin antagonist (Murata et al. 2011; De Bond et al. 2013). We therefore hypothesized that the arcuate kisspeptin system may also respond to female chemosignals in male hamsters. Considering expression of kisspeptin in this region is regulated by photoperiod at least somewhat independently from changes in steroid hormones (Revel et al. 2006; Ansel et al. 2010), this population also seemed a promising candidate for photoperiodic gating of neuroendocrine responses. FHVS exposure did not cause changes in kisspeptin-ir fiber density in this region, but we were unfortunately unable to quantify the activational state of this population due to intense fiber staining obscuring cell bodies. Not unexpectedly, the current study detected no differences within the AVPV kisspeptin population after FHVS exposure. This population is implicated in sex steroid positive feedback and the control of ovulation in females (see Kriegsfeld [2013] for review), but is much smaller in males and has previously been found to be unresponsive to same- and opposite-sex exposure in mice (Szymanski and Keller 2014; Taziaux and Bakker 2015; Jennings et al. 2016).

Taken together, the present study identifies the POA and the RFRP neuronal system as important centers for the integration of photoperiodic and chemosensory information. Responses within these systems to female chemosignals are gated seasonally, and responsiveness is not rescued by T replacement in SD animals. These results mirror photoperiodic regulation of behavioral and neuroendocrine responses to female chemosignals (Morin and Zucker 1978; Miernicki et al. 1990; Anand et al. 2002). Thus, changes within the POA and RFRP neuronal system present a likely means by which photoperiod regulates processing of chemosensory cues to restrict reproduction to the appropriate season.

## Acknowledgments

We thank Jenny Chang, Miranda Theriot, and the UC Berkeley Office of Laboratory and Animal Care for their technical assistance.

## Funding

This work was supported by the National Institute of Health [grant HD-050470 to L.J.K.], National Science Foundation [grant IOS-1257638 to L.J.K.], and The University of California France-Berkeley Fund [to L.J.K. and M.K.].

## References

Anand S, Losee-Olson S, Turek FW, Horton TH. 2002. Differential regulation of luteinizing hormone and follicle-stimulating hormone in male siberian hamsters by exposure to females and photoperiod. Endocrinology 143:2178–88.

Ancel C, Bentsen AH, Sebert ME, Tena-Sempere M, Mikkelsen JD, Simonneaux V. 2012. Stimulatory effect of RFRP-3 on the gonadotrophic axis in the male Syrian hamster: the exception proves the rule. Endocrinology 153:1352–63.

Ansel L, Bolborea M, Bentsen AH, Klosen P, Mikkelsen JD, Simonneaux V. 2010. Differential regulation of kiss1 expression by melatonin and gonadal hormones in male and female Syrian hamsters. J Biol Rhythms 25:81–91.

Bentley GE, Jensen JP, Kaur GJ, Wacker DW, Tsutsui K, Wingfield JC. 2006. Rapid inhibition of female sexual behavior by gonadotropin-inhibitory hormone (GnIH). Horm Behav 49:550–5.

Calisi RM, Diaz-Munoz SL, Wingfield JC, Bentley GE. 2011. Social and breeding status are associated with the expression of GnIH. Genes Brain Behav 10:557–64.

Campbell CS, Finkelstein JS, Turek FW. 1978. The interaction of photoperiod and testosterone on the development of copulatory behavior in castrated male hamsters. Physiol Behav 21:409–15.

Clarke IJ, Caraty A. 2013. Kisspeptin and seasonality of reproduction. Adv Exp Med Biol 784:411–30.

Coolen LM, Wood RI. 1998. Bidirectional connections of the medial amygdaloid nucleus in the Syrian hamster brain: simultaneous anterograde and retrograde tract tracing. J Comp Neurol 399:189–209.

d'Anglemont de Tassigny X, Fagg LA, Carlton MB, Colledge WH. 2008. Kisspeptin can stimulate gonadotropin-releasing hormone (GnRH) release by a direct action at GnRH nerve terminals. Endocrinology 149:3926–32.

Darby EM, Devor M, Chorover SL. 1975. A presumptive sex pheromone in the hamster: some behavioral effects. J Comp Physiol Psychol 88:496–502.

De Bond JA, Li Q, Millar RP, Clarke IJ, Smith JT. 2013. Kisspeptin signaling is required for the luteinizing hormone response in anestrous ewes following the introduction of males. PLoS One 8:e57972.

de Roux N, Genin E, Carel JC, Matsuda F, Chaussain JL, Milgrom E. 2003. Hypogonadotropic hypogonadism due to loss of function of the KiSS1-derived peptide receptor GPR54. Proc Natl Acad Sci U S A 100:10972–6.

Fiber JM, Adames P, Swann JM. 1993. Pheromones induce c-fos in limbic areas regulating male hamster mating behavior. Neuroreport 4:871–4.

Fiber JM, Swann JM. 1996. Testosterone differentially influences sex-specific pheromone-stimulated Fos expression in limbic regions of Syrian hamsters. Horm Behav 30:455–73.

Gaston S, Menaker M. 1967. Photoperiodic control of hamster testis. Science 158:925–8.

Gore AC, Wersinger SR, Rissman EF. 2000. Effects of female pheromones on gonadotropin-releasing hormone gene expression and luteinizing hormone release in male wild-type and oestrogen receptor-alpha knockout mice. J Neuroendocrinol 12:1200–4.

Hull EM, Dominguez JM. 2007. Sexual behavior in male rodents. Horm Behav 52:45–55.

Irwig MS, Fraley GS, Smith JT, Acohido BV, Popa SM, Cunningham MJ, Gottsch ML, Clifton DK, Steiner RA. 2004. Kisspeptin activation of gonadotropin releasing hormone neurons and regulation of KiSS-1 mRNA in the male rat. Neuroendocrinology 80:264–72.

Jennings KJ, Chang J, Cho H, Piekarski DJ, Russo KA, Kriegsfeld LJ. 2016. Aggressive interactions are associated with reductions in RFamide-related peptide, but not kisspeptin, neuronal activation in mice. Horm Behav 78:127–34.

Johnson MA, Tsutsui K, Fraley GS. 2007. Rat RFamide-related peptide-3 stimulates GH secretion, inhibits LH secretion, and has variable effects on sex behavior in the adult male rat. Horm Behav 51:171–80.

Johnston RE. 1974. Sexual attraction function of golden hamster vaginal secretion. Behav Biol 12:111–7.

Jouhanneau M, Szymanski L, Martini M, Ella A, Keller M. 2013. Kisspeptin: a new neuronal target of primer pheromones in the control of reproductive function in mammals. Gen Comp Endocrinol 188:3–8.

Kriegsfeld LJ. 2013. Circadian regulation of kisspeptin in female reproductive functioning. In: Kauffman AS, Smith JT, editors. Kisspeptin signaling in reproductive biology. New York (NY): Springer. p. 385–410.

Kriegsfeld LJ, Bittman EL. 2009. Photoperiodism and reproduction in mammals. In: Nelson RJ, Denlinger DL, Somers DE, editors. Photoperiodism: the biological calendar. New York (NY): Oxford University Press. p. 503–42.

Kriegsfeld LJ, Mei DF, Bentley GE, Ubuka T, Mason AO, Inoue K, Ukena K, Tsutsui K, Silver R. 2006. Identification and characterization of a gonadotropin-inhibitory system in the brains of mammals. Proc Natl Acad Sci U S A 103:2410–5.

Lehman MN, Hileman SM, Goodman RL. 2013. Neuroanatomy of the kisspeptin signaling system in mammals: comparative and developmental aspects. In: Kauffman AS, Smith JT, editors. Kisspeptin signaling in reproductive biology. New York (NY): Springer. p. 27–62.

Liberles SD. 2014. Mammalian pheromones. Annu Rev Physiol 76:151–75.

Lisk RD, Ciaccio LA, Catanzaro C. 1983. Mating behaviour of the golden hamster under seminatural conditions. Anim Behav 31:659–66.

Losa SM, Todd KL, Sullivan AW, Cao J, Mickens JA, Patisaul HB. 2011. Neonatal exposure to genistein adversely impacts the ontogeny of hypothalamic kisspeptin signaling pathways and ovarian development in the peripubertal female rat. Reprod Toxicol 31:280–9.

Macrides F, Bartke A, Fernandez F, D'Angelo W. 1974. Effects of exposure to vaginal odor and receptive females on plasma testosterone in the male hamster. Neuroendocrinology 15:355–64.

Mason AO, Duffy S, Zhao S, Ubuka T, Bentley GE, Tsutsui K, Silver R, Kriegsfeld LJ. 2010. Photoperiod and reproductive condition are associated with changes in RFamide-related peptide (RFRP) expression in Syrian hamsters (*Mesocricetus auratus*). J Biol Rhythms 25:176–85.

Maywood ES, Bittman EL, Hastings MH. 1996. Lesions of the melatonin- and androgen-responsive tissue of the dorsomedial nucleus of the hypothalamus block the gonadal response of male Syrian hamsters to programmed infusions of melatonin. Biol Reprod 54:470–7.

Miernicki M, Pospichal MW, Powers JB. 1990. Short photoperiods affect male hamster sociosexual behaviors in the presence and absence of testosterone. Physiol Behav 47:95–106.

Morin LP, Wood RI. 2001. A stereotaxic atlas of the golden hamster brain. San Diego (CA): Academic Press.

Morin LP, Zucker I. 1978. Photoperiodic regulation of copulatory behaviour in the male hamster. J Endocrinol 77:249–58.

Murata K, Wakabayashi Y, Sakamoto K, Tanaka T, Takeuchi Y, Mori Y, Okamura H. 2011. Effects of brief exposure of male pheromone on multiple-unit activity at close proximity to kisspeptin neurons in the goat arcuate nucleus. J Reprod Dev 57:197–202.

Murphy MR. 1973. Effects of female hamster vaginal discharge on the behavior of male hamsters. Behav Biol 9:367–75.

Murphy MR, Schneider GE. 1970. Olfactory bulb removal eliminates mating behavior in the male golden hamster. Science 167:302–4.

Nyby JG. 2008. Reflexive testosterone release: a model system for studying the nongenomic effects of testosterone upon male behavior. Front Neuroendocrinol 29:199–210.

Peragine DE, Pokarowski M, Mendoza-Viveros L, Swift-Gallant A, Cheng HM, Bentley GE, Holmes MM. 2017. RFamide-related peptide-3 (RFRP-3) suppresses sexual maturation in a eusocial mammal. Proc Natl Acad Sci U S A 114:1207–12.

Peters KD, Hom SM, Wood RI. 2004. Testosterone and chemosensory detection in male Syrian hamster. Horm Behav 46:341–8.

Petrulis A. 2013. Chemosignals, hormones and mammalian reproduction. Horm Behav 63:723–41.

Pfeiffer CA, Johnston RE. 1994. Hormonal and behavioral responses of male hamsters to females and female odors: roles of olfaction, the vomeronasal system, and sexual experience. Physiol Behav 55:129–38.

Piekarski DJ, Zhao S, Jennings KJ, Iwasa T, Legan SJ, Mikkelsen JD, Tsutsui K, Kriegsfeld LJ. 2013. Gonadotropin-inhibitory hormone reduces sexual motivation but not lordosis behavior in female Syrian hamsters (*Mesocricetus auratus*). Horm Behav 64:501–10.

Pospichal MW, Karp HD, Powers JB. 1991. Influence of daylength on male hamster sexual behavior: masking effects of testosterone. Physiol Behav 49:417–22.

Powers JB, Bergondy ML. 1983. Androgenic regulation of chemoinvestigatory behaviors in male and female hamsters. Horm Behav 17:28–44.

Revel FG, Saboureau M, Masson-Pevet M, Pevet P, Mikkelsen JD, Simonneaux V. 2006. Kisspeptin mediates the photoperiodic control of reproduction in hamsters. Curr Biol 16:1730–5.

Revel FG, Saboureau M, Pevet P, Simonneaux V, Mikkelsen JD. 2008. RFamide-related peptide gene is a melatonin-driven photoperiodic gene. Endocrinology 149:902–12.

Richardson HN, Nelson AL, Ahmed EI, Parfitt DB, Romeo RD, Sisk CL. 2004. Female pheromones stimulate release of luteinizing hormone and testosterone without altering GnRH mRNA in adult male Syrian hamsters (*Mesocricetus auratus*). Gen Comp Endocrinol 138:211–7.

Romeo RD, Parfitt DB, Richardson HN, Sisk CL. 1998. Pheromones elicit equivalent levels of Fos-immunoreactivity in prepubertal and adult male Syrian hamsters. Horm Behav 34:48–55.

Sakamoto K, Wakabayashi Y, Yamamura T, Tanaka T, Takeuchi Y, Mori Y, Okamura H. 2013. A population of kisspeptin/neurokinin B neurons in the arcuate nucleus may be the central target of the male effect phenomenon in goats. PLoS One 8:e81017.

Sisk CL, Turek FW. 1983. Developmental time course of pubertal and photoperiodic changes in testosterone negative feedback on gonadotropin secretion in the golden hamster. Endocrinology 112:1208–16.

Smith JT, Young IR, Veldhuis JD, Clarke IJ. 2012. Gonadotropin-inhibitory hormone (GnIH) secretion into the ovine hypophyseal portal system. Endocrinology 153:3368–75.

Swann JM. 1997. Gonadal steroids regulate behavioral responses to pheromones by actions on a subdivision of the medial preoptic nucleus. Brain Res 750:189–94.

Szymanski LA, Keller M. 2014. Activation of the olfactory system in response to male odors in female prepubertal mice. Behav Brain Res 271:30–8.

Taziaux M, Bakker J. 2015. Absence of female-typical pheromone-induced hypothalamic neural responses and kisspeptin neuronal activity in alpha-fetoprotein knockout female mice. Endocrinology 156:2595–607.

Tobari Y, Son YL, Ubuka T, Hasegawa Y, Tsutsui K. 2014. A new pathway mediating social effects on the endocrine system: female presence acting via norepinephrine release stimulates gonadotropin-inhibitory hormone in the paraventricular nucleus and suppresses luteinizing hormone in quail. J Neurosci 34:9803–11.

Tsutsui K, Saigoh E, Ukena K, Teranishi H, Fujisawa Y, Kikuchi M, Ishii S, Sharp PJ. 2000. A novel avian hypothalamic peptide inhibiting gonadotropin release. Biochem Biophys Res Commun 275:661–7.

Ubuka T, Bentley GE, Ukena K, Wingfield JC, Tsutsui K. 2005. Melatonin induces the expression of gonadotropin-inhibitory hormone in the avian brain. Proc Natl Acad Sci U S A 102:3052–7.

Ubuka T, Haraguchi S, Tobari Y, Narihiro M, Ishikawa K, Hayashi T, Harada N, Tsutsui K. 2014. Hypothalamic inhibition of socio-sexual behaviour by increasing neuroestrogen synthesis. Nat Commun 5:3061.

Ubuka T, Inoue K, Fukuda Y, Mizuno T, Ukena K, Kriegsfeld LJ, Tsutsui K. 2012. Identification, expression, and physiological functions of Siberian hamster gonadotropin-inhibitory hormone. Endocrinology 153:373–85.

Whalen RE, Debold JF. 1974. Comparative effectiveness of testosterone, androstenedione and dihydrotestosterone in maintaining mating behavior in the castrated male hamster. Endocrinology 95:1674–9.

Wood RI, Newman SW. 1995. Integration of chemosensory and hormonal cues is essential for mating in the male Syrian hamster. J Neurosci 15:7261–9.

Yeo SH, Herbison AE. 2011. Projections of arcuate nucleus and rostral periventricular kisspeptin neurons in the adult female mouse brain. Endocrinology 152:2387–99.

Zucker I, Morin LP. 1977. Photoperiodic influences on testicular regression, recrudescence and the induction of scotorefractoriness in male Golden hamsters. Biol Reprod 17:493–8.